

Design, Modeling and Simulation of Axial Flux Permanent Magnet Synchronous Machine for Electric Vehicles

LARBI B^{1,3}, HATTI M², KOUZI K³, GHADBANE A¹

¹Research Nuclear Center of Birine CRNB Box 180, Ain Oussera, ALGERIA

²Research Center in Renewable Energy, Bousmail, ALGERIA

³Electrical Department; University Amar Telidji of LAGHOUAT, ALGERIA

Abstract - Studies, most of the pollution from urban areas comes from vehicle emissions and the explosive growth in the number of vehicles. Therefore, finding a solution to reduce (or eliminate) pollution is a vital need. If in public transport (trains, buses and trams) there are non-polluting solutions (electric), for individual transport the electrification of vehicles is one of the solutions implemented by car manufacturers.

The Axial Flux and Permanent Magnet Machine (MFAP) represent a serious candidate for electric traction because of its high density and mass density of torque. In this paper presented the design of Low Speed Flux Permanent (AFPM) Machine with Non-Slotted TORUS-NS topology type. The aim of the study is to provide the flux density in the model particularly at the Air-gap by numerical procedure. Field analysis of the slotless machine (AFPM) is investigated using Finite Element method (FEM). The model of the machine was implemented on the commercial code Maxwell 16.0. The result obtained is illustrated and in the paper and numerical quality is relatively good agreement with those of literature,

Key Words: Axial Flux Permanent Magnet (AFPM) Machine; Finite Element Method (FEM) 2D; TORUS NS.

1. INTRODUCTION

drives have been progressively penetrating for more than a century all areas of society (in developed countries they consume about a quarter of total electricity consumption and over 70% of consumption industrial [1]). In most cases, the load is driven via a more or less complex mechanical transmission: gearbox, multiplier, rack pinion, differential, universal joints ... The transmission then has the role of adapting the load to the engine, which allows to use, more often than not, standard motors. The mechanical transmission also allows, in many situations, to move the engine to a place where more space is available. In a growing number of applications, for various reasons that we will try to highlight, it is desired to directly transmit the forces to the mechanical load. This is called direct training. The necessary actuators are then designed according to particular criteria, to integrate better in the system, to produce high torque at low speed, to work at very high speeds, to produce linear movements or to produce large accelerations. This trend towards the simplification of the transmission chain goes in the direction of the improvement of the reliability by the reduction of the number of links of this chain but the constraints of cost, always primordial, often limit the

penetration of these techniques. [2] Significant developments have occurred in recent years thanks to advances in the field of materials (magnetic, mechanical or thermal ...), conversion principles, power electronics (higher power, higher frequencies, new architectures ...), control (digital technologies and new methods of the automatic), sensors and structures (creativity of the designers) the motors AFPM are of crepe type, adapt perfectly to the wheel of a motor vehicle and, of this fact, can be easily and compactly integrated into the wheel. According to these properties, axial flow motors seem to be a better choice than more conventional radial flow motors for this type of application. We illustrate in this article a concept, or a synchronous machine with permanent magnet can further eliminate the need for a gearbox **Fig -1**

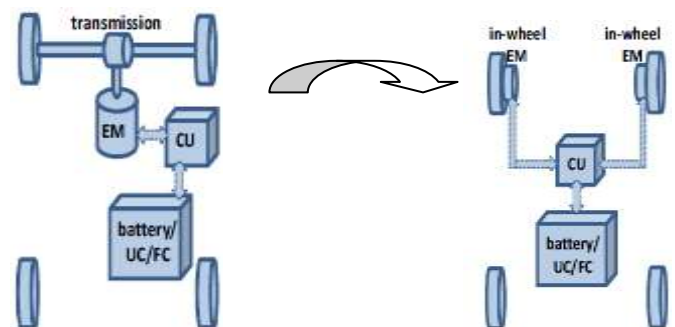


Fig -1: Description of the targeted PM drive

2. AXIAL FLUX PERMANENTMAGNET MACHINE

2.1 Presentation of the Axial Machine

We give the following schematic representation of the axial flux machines, as compared to radial flux machines. The rotor of a rotary machine involves the creation of a couple, so a force in the direction orthoradial to the axis of rotation. Assuming that the forces in the electrical machines are due to Lorentz forces, there are two ways to generate these forces in the orthoradial direction.

The first is to guide the induction in the radial direction (called radial flux machine) [3] with the currents in the axial direction (Figure 2.a), the force being good in this case in the management orthoradial. The second method to generate a force in the direction of orthoradial is to place the induction in the axial direction; the currents are in turn in the radial direction (Figure 2b).

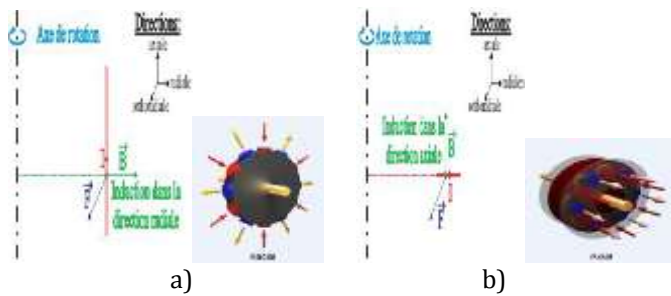


Fig -2: Principle of operation of the machine
a) radial flux b) axial flow

2.2 Topologies of the Axial Machine

One of the most interesting aspects of axial flux machines is the wide range of topologies they offer. These different options may fit several applications. In [9] a deep study of the different topologies of axial flux machines is done. As shown in Figure 1-3, axial flux machines are divided into three main groups: single-side machines (Fig. 4), double side machines (Fig. 5 and Fig. 6) and multistage machines (Fig. 7). In addition, a variety of configurations can be carried out within each group. This constructive flexibility makes axial machines suitable for different applications and optimizable for the specific requirements of each application.

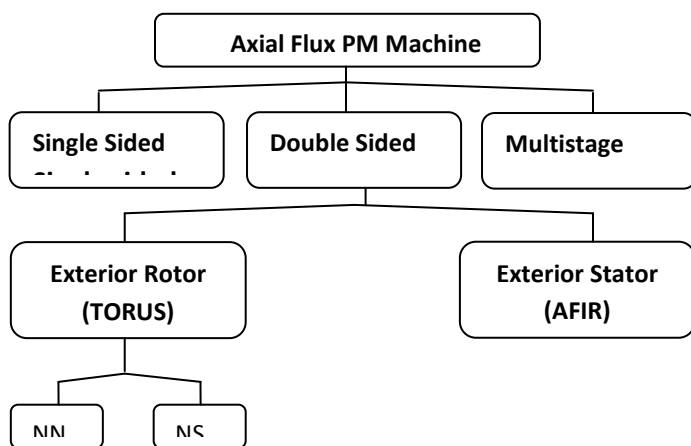


Fig -3: Diagram of axial machine topologies

2.2.1 Single-rotor single-stator axial-flux permanent magnet

This is the simplest topology in the axial flux machines range. This kind of machine consists of a single stator and a single rotor, as shown in Fig.4. The stator core may be either slotted (Fig.4-a) or slotless (Fig.4-b).

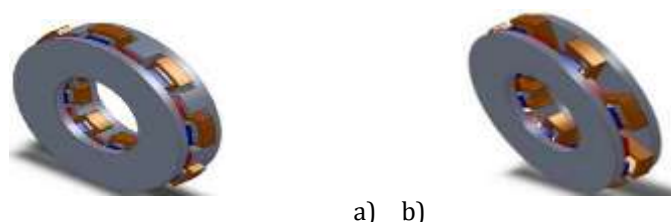


Fig -4: Single side machine: a) slotted stator and b) slotless stator

In this configuration, the attraction force exerted by the magnets between the rotor and the stator may be a drawback. The axle and the bearings must withstand this force, so they have to be properly dimensioned.

2.2.2 Double Side axial-flux permanent magnet

Double side machines consist of three elements in two possible configurations:

- Double Stator – Single Rotor: The interior rotor is placed between two stators.
- Single Stator – Double rotor: The interior stator is placed between two rotors.

a) Single-rotor double-stator axial-flux permanent magnet (AFIR):

In these kinds of machines, an interior rotor is placed between two stators, as shown in Fig.5. One of the interesting advantages of this configuration is that the core of the rotor shown in Fig.5-a can be avoided to obtain a coreless rotor as shown in Fig.5-b. The magnets have to be held in a non-ferromagnetic material to create the rotor structure. In this way, a lighter machine is obtained. It has to be noted that because the rotor is between the two stators and in the case when the distance from the rotor to each stator is equal, the attraction forces are equilibrated, avoiding possible stress in mechanical parts

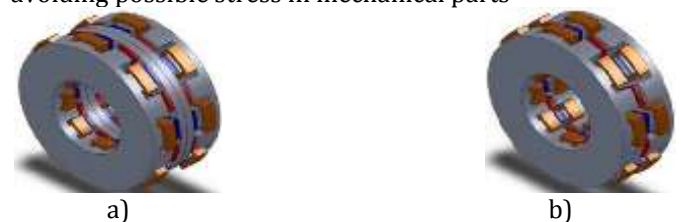


Fig-5: Interior rotor machines: a) with ferromagnetic core in the rotor and b) coreless rotor

Similar to single side machines, the stators can be either slotted or slotless. The electrical connection between the two stators may in series or parallel, taking into account that the characteristics of the machine depend on this connection: that is, higher voltage in a series connection and higher current in a parallel connection.

b) Double-rotor single-stator axial-flux permanent magnet (TORUS):

In this topology, the magnets are usually mounted in a ferromagnetic material to facilitate the magnetic flux flow between adjacent magnets. There is a wide range of possibilities for the configuration of the stators in these machines. On the one hand, in the configuration known as north-north (N-N), magnets with opposite magnetization direction are placed in front of each other, as shown in Fig. 6. In this configuration, the path of magnet flux is closed along the stator yoke so that the stator core is needed. The winding may be placed surrounding the teeth, as shown in Fig.6-a. This figure shows a slotted stator with concentrated one layer winding. However, a toroidal winding with a slotless

stator would be also possible, as shown in Fig.6-b. The main disadvantage of slotless machines is that the coils take place in the air gap, which increases the effective air gap length.

Another possible configuration is the north-south (N-S) machine. In this case, magnets with the same magnetization direction are placed in front of each other. The magnetic flux passes through the air gap and is then closed through the rotor yoke. Because the path followed by the flux does not use the stator yoke, this part could be avoided, leading to a lighter stator core consisting only of ferromagnetic teeth, as shown in Fig.6-c. Moreover, it could even be possible to avoid the whole stator core and place the coils in the air gap as shown in Fig.6-d. However, the N-S configuration is not feasible with toroidal windings because both side forces would cancel each other, resulting in a null overall torque.)

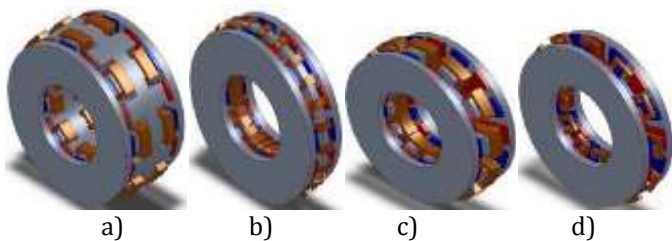


Fig-6: a) Interior slotted stator N-N machine with lap winding, b) Interior slotless stator NN machine toroidal winding, c) Interior ferromagnetic core stator N-S machine, and b) Interior coreless stator N-S machine

c) Multi-rotor multi-stator AFPM

This topology could be defined more accurately as a concept than a type of machine. The idea is to place stators and rotors alternately to obtain a machine with as much sides or stages as desired in order to fulfill the application’s requirements. This configuration offers a quite interesting possibility: modularity. Fig.7 shows a multistage axial machine with two stators and three rotors. The connection between the winding of different stages could be done in either series or parallel. Furthermore, a connection/disconnection of stages could be done depending on the temporary requirements of the application. This connection may allow fault tolerance as the machine can keep working even if any of the stages is damaged or disconnected.

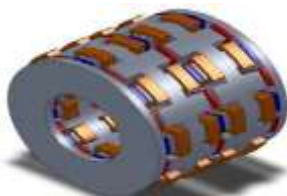


Fig-7: Multistage axial flux machine with two stators and three rotors

3. MODELING AND SIMULATION OF THE AFPM MACHINE

3.1 Machine structure of case study

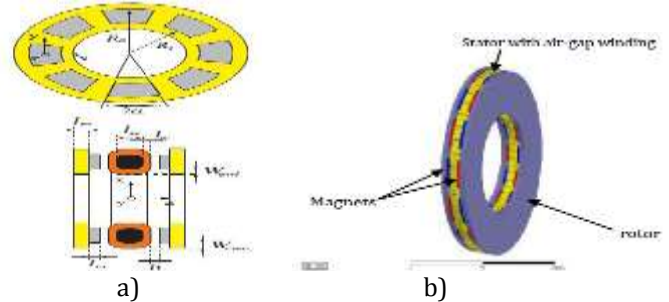


Fig-8: a) Definition of the geometrical parameters for the TORUS-NS AFPM machines [6] b) Axial flux TORUS type non-slotted surface mounted PM machine configuration (TORUS-NS)

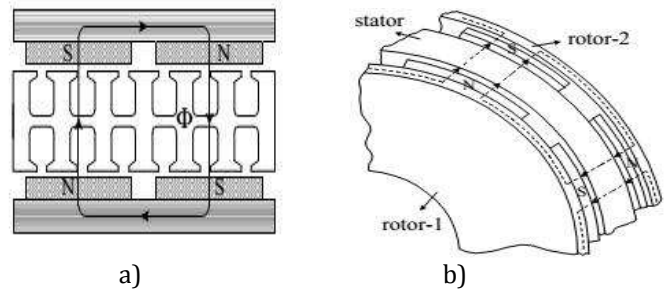


Fig-9: PM polarities and magnetic flux paths of a TORUS-NS machine [7] a) 2D b) 3D

3.2 Sizing equation for the AFPM machine

The design is in several steps. The first is to choose the configuration, that is, the number of phases, magnets and slots. Then, the main dimensions of each electrical machine are determined through electrical-machine output power equation. Assuming negligible leakage inductance and resistance, rated power is expressed as:

$$K_p = \frac{1}{T} \int_0^T \frac{e(t) \times i(t)}{E_{pk} \times I_{pk}} dt = \frac{1}{T} \int_0^T f_e(t) \cdot f_i(t) dt \tag{1}$$

$e(t)$ is phase air-gap EMF, $i(t)$ is phase current, η is machine efficiency, m is number of machine phases and T period of one cycle EMF. A general-purpose sizing equation for AFPM machines has been provided by other authors previous literatures [7]. For an AFPM machine, it takes the following form:

$$K_i = \frac{I_{pk}}{I_{rms}} = \frac{1}{\sqrt{\frac{1}{T} \int_0^T \left(\frac{i(t)}{I_{pk}}\right)^2 dt}} \tag{2}$$

Here I_{rms} is the root mean square (rms) of the phase current. The peak value of the phase air-gap of EMF for the AFPM machine in (1) is expressed as:

$$E_{pk} = K_e N_{ph} B_g \frac{f}{p} (1 - \lambda^2) D_0^2 \tag{3}$$

K_e is the EMF factor that incorporates the winding distribution factor (K_w) and per-unit portion of the air-gap area covered by the salient poles of the machine (if any); N_{ph} is the number of winding turns per phase; B_g is the flux density in the air gap; f is the converter frequency; p is the machine pole pairs; λ is the diameter ratio equal to D_i/D_o which D_i is the outer surface diameter and D_o is the inner surface diameter of the AFPM machine. The peak phase current for (1) is expressed as:

$$I_{pk} = A\pi K_i \frac{1+\lambda}{2} \cdot \frac{D_o}{2m_1 N_{ph}} \quad (4)$$

Where m_1 is the number of phases, and A is the total electrical loading. The sizing equation for AFPM machines is presented as:

$$P_s = \frac{1}{1+K_g} \frac{m}{m_1} \frac{\pi}{2} K_s K_i K_p K_L \eta B_g A \frac{f}{p} (1-\lambda^2) \frac{1+\lambda}{2} D_1^2 L_s \quad (5)$$

k_s is the electrical loading ratio on the rotor and stator; and K_L is the aspect ratio coefficient of a specific machine structure that considers the consequence of loss, temperature rise, and design efficiency requirements. The machine torque density for the total volume is defined as:

$$\tau_{dem} = \frac{P_{out}}{\omega_{m_4} \frac{\pi}{4} D_{tot}^2 L_{tot}} \quad (6)$$

3.3 Simulation Result

Two-dimensional (2D) electromagnetic analysis of the machine structure axial flux with permanent magnets is necessary, in order to determine a topology optimal machine for our application, to have analytical models sufficiently accurate and fast. The 2D hypothesis appears natural when one is working on the analytical modeling of electrical machines, because it allows to considerably facilitating the equation of the problem [9, 10].

Note that FEM (Finite Element Method) facilitates the analysis of problems with respect to the electromagnetic field for complex geometric configurations [11-12]. The digital model of the synchronous machine TOURIS NS has been simulated under the ANSYS MAXWELL 16.0 commercial software [13]. The different parameters and model specifications are shown in the table (Appendix). Meshing is an indispensable step in numerical modeling. A bad mesh can generate erroneous results. This is why it is important to develop a mesh that respects a compromise between finesse and computation time. Figure 9 shows the typical mesh of the model chosen.

The different parameters and model specifications are shown in the table I; II (lists the motor's design dimensions and specifications).

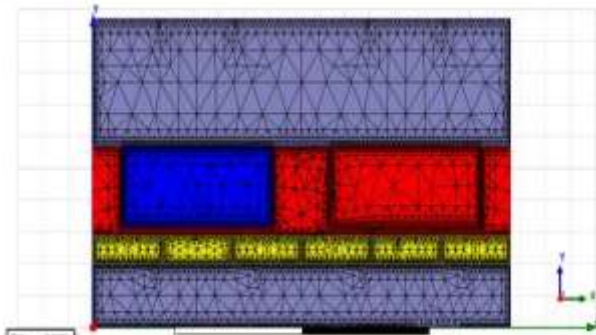
Table-1: Selected values of principal design details

Symbol	Quantity	Value	Unit
P_R	Nominal power	5000	[W]
m	Number of phase	3	-
V_{DC}	DC Voltage	210	[V]
f	frequency	46.67	[Hz]
n	Nominal speed	200	[rpm]
connexion			Y

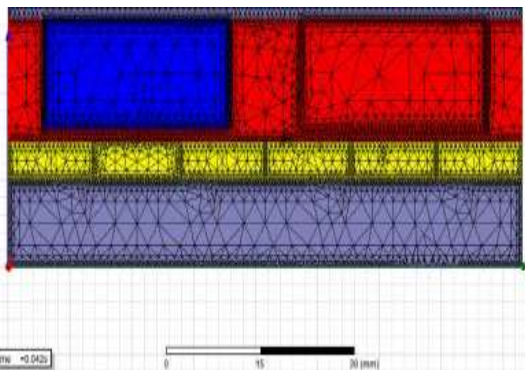
Table-2: Analytically Designed Parameter of TORUS-NS AFPM Machine

Symbol	Quantity	Value	Unit
V_L	Line Voltage	219.05	[V]
V_P	Phase Voltage	126.47	[V]
p	Number of pole pair	14	-
A	Electrical Loading	10500	[A/m]
J	Current Density]	7.8]
aP	Number of parallel path	7	A/m
B_g	Air-gap peak flux density	0.74	m ²
λ	Diameter ratio	0.5745	-
K_p	Electrical power waveform factor	0.777	[T]
	Current waveform factor		-
K_i	EMF factor	0.134	-
K_e	Copper fill factor	Π	-
K_{cu}	PM Magnetic recoil permeability -	0.33	-
μ_{rPM}	residual flux density of the PM	1.05	-
B_r	material	1.17	-
	Flux density in the rotor core		-
B_{cr}	Leakage flux factor	1.17	[T]
K_d	Specific magnetic loading	0.533	[T]
B_u	Efficiency	1.125	-
η	Outer Diameter	0.81	[T]
D_o	Inner Diameter	0.470	-
D_i	Average Diameter	0.270	[m]
Dg	Air-gap length (magnet to the	0.370	[m]
g	winding)	0.0015	[m]
	Flux density in the stator core		[m]
B_{cs}	Axial length of the stator core	1.245	[T]
L_{cs}	Winding thickness at inner	0.020	[m]
W_{cui}	diameter	0.0055	[m]
W_{cwo}	Winding thickness at outer	0.0032	[m]
	diameter		
W_{cu}	Winding thickness at inner diameter	0.0043	[m]
L_s	axial length of the stator	0.0288	[m]
L_{cr}	axial length of the rotor core	0.020	[m]
LPM	PM length	0.0127	[m]
α_i	magnet width-to-pole pitch ratio	0.72	-
w_{PMg}	Magnet width in average diameter	0.0299	[m]
L_r	axial length of the rotor	0.0327	[m]
L_e	axial length of the machine	0.097	[m]
N_t	number of turns per phase	160	Turn
I_{ef}	RMS phase current	12.71	[A]
lw	axial thickness of the winding	0.0044	[m]
sa	cross-section of a conductor	0.329	[m ²]
d_{str}	Strand wire diameter	0.71	[m]
Li	effective length of the stack	0.1	[m]
L_{lav}	Average length of the armature turn	0.2576	[m]

Meshing is an indispensable step in numerical modeling. A bad mesh can generate erroneous results. This is why it is important to develop a mesh that respects a compromise between finesse and computation time. Figure 9 shows the typical mesh of the model chosen.

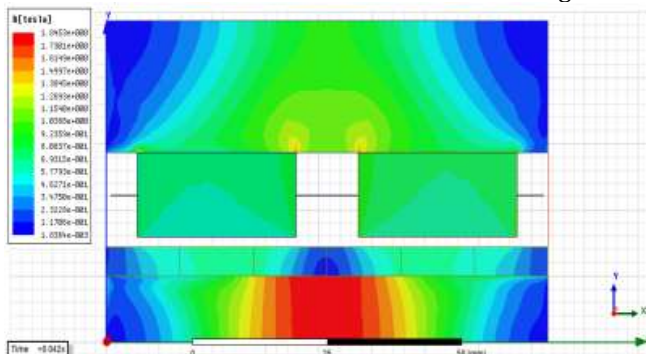


a) mesh of the studied structure

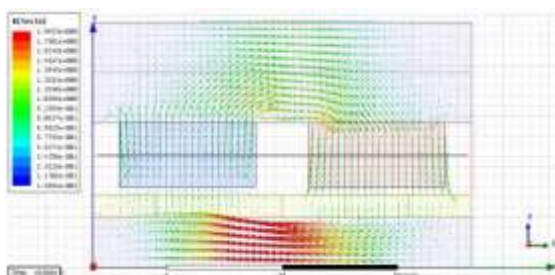


b) mesh view of the gap zone.

Fig-10: Mesh of the TORUS NS machine The distribution of flux density by means of vectors and flow direction to know the state without load is shown in the figure



a) vector of magnetic flux density



b) magnetic flux paths

Fig-11: Magnetic flux density

The air gap flux density under a pole using MEF analysis. We can see from this curve that the ratio of the maximum flow density gap is about 0.749 T and the average flux density of air gap is determined at 0.67 T.

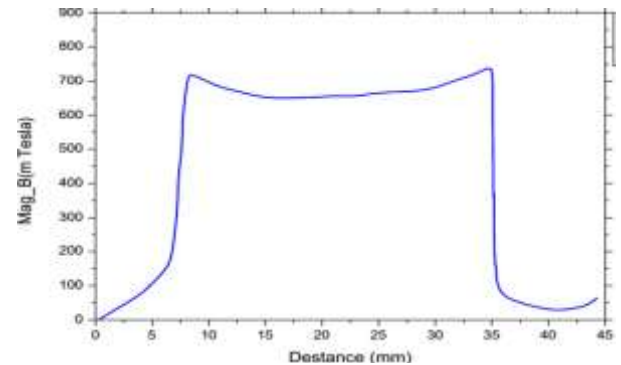


Fig-12: Magnetic flux density of air gap under a pole (at medium diameter $D_g = (D_i + D_o) / 2$)

4. CONCLUSION

This paper presents the design process for a TORUS axial-flow axial magnet permanent magnet motor, suitable for direct driving an electric vehicle using the design equation and finite element analysis. The AFPM engine is a high torque motor that can be easily and compactly mounted in the wheel of the car by perfectly adjusting the rim. An AFPM motor with double-sided rotor slots for high torque density and stable rotation is the preliminary design. To determine design requirements. The fundamental theory and sizing equation of the axial flux permanent magnet machine are applied to obtain the initial design parameters of the motor with the highest possible torque. The results of the FEA simulation are compared with the results obtained from the sizing equation showing good agreement of the flux density values in various parts of the engine designed to be empty. The engine meets all the requirements and limitations of the electric vehicle adapting to the shape and size of a conventional rim of the vehicle wheel.

REFERENCES

- [1] B. MULTON, « L'énergie sur la terre : analyse des ressources et de la consommation. La place de l'énergie électrique. », Revue 3E. In°13, septembre98, 9p.
- [2] B. MULTON, J. BONAL " Les entrainement électromagnétique direct" 4 février 1999 -ENS Cachan – SEE
- [3] O. de la Barrière «Modèles analytiques électromagnétiques bi et tri dimensionnels en vue de l'optimisation des actionneurs disques. Etude théorique et expérimentale des pertes, magnétiques dans les matériaux granulaires
- [4] J. F. Gieras, R. J. Wang, and M. J. Kamper, Axial Flux Permanent Magnet Brushless Machines. Kluwer Academic Publishers, 2004
- [5] B.J. Chalmers, Wu Wei, E. Spooner, "An Axial-Flux

Permanent-Magnet Generator for a Gearless Wind Energy System", IEEE Int. Conf. on Power Electronic Drives and Energy Systems for industrial Growth, PEDESP6, New Delhi, pp. 610-616.

- [6] F. Libert, "Design, Optimization and Comparison of Permanent Magnet Motors for a Low-Speed Direct-Driven Mixer", Licentiate Thesis, Royal Institute of Technology, Stockholm 2004
- [7] Surong Huang, Metin Aydin Thomas A. Lipo "TORUS Concept Machines: Pre-Prototyping Design Assessment for Two Major Topologies"; IEEE International Conference on Electrical Machines and Drives, Boston, 2001, pp.645-651.
- [8] Gonzalez-Lopez, D., Tapia, J., Wallace, R. et Valenzuela, A. (2008). Design and test of AFPM with field control capability. IEEE Trans. on Magnetics, 44(9):2168-2173.
- [9] Liu, C. T. and S. C. Lee, "Magnetic field modeling and optimal operational control of a single-side axial-flux permanent magnet motor with center poles," Journal of Magnetism and Magnetic Materials, Vol. 304, No. 1, 454-456, September 2006
- [10] Liu, C. T., S. C. Lin, and T. S. Chiang, "On the analytical flux distribution modeling of an axial-flux surface-mounted permanent magnet motor for control applications," Journal of Magnetism and Magnetic Materials, Vol. 282, 346-350, November 2004
- [11] Vaseghi, B., N. Takorabet, and F. Meibody-Tabar, "Transient finite element analysis of induction machines with stator winding turn fault," Progress In Electromagnetic Research, Vol. 95, 1-18, 2009.
- [12] Torkaman, H. and E. Afjei, "Comparison of two types of dual layer generator in field assisted mode utilizing 3D-FEM and experimental verification," Progress In Electromagnetics Research B, Vol. 23, 293-309, 2010
- [13] ANSYS MAXWELL Version 16.0 user's guide – Maxwell 3D, 2010
- [14] <http://www.ansys.com>